MAPPING THE SOLAR WIND FROM ITS SOURCE REGION INTO THE OUTER CORONA

NASA Grant NAG5-6192

Final Report

For the period 1 August 1997 through 31 July 2000

Principal Investigator

Ruth Esser

November 2000

Prepared for

National Aeronautics and Space Administration

Washington, D.C. 20546

Smithsonian Institution
Astrophysical Observatory
Cambridge, Massachusetts 02138

The Smithsonian Astrophysical Observatory
is a member of the
Harvard-Smithsonian Center for Astrophysics

The NASA Technical Officer for this Grant is Dr. William J. Wagner, 078.0 Code SR, NASA Headquarters, Washington, DC 20546.

Final Report for the grant "Mapping the Solar Wind from Its Source Region into the Outer Corona", NAG5-6192

For the Period August 1. 1997 to July 31. 2000

1. Summary

1.1 Scope of the Investigation

The solar wind not only forms the space environment of earth and other planets, but is also the cause of many phenomena observed in the earth's atmosphere, such as aurorae. The expansion of the coronal plasma of the Sun is characteristic to many main sequence stars, and thus provides an example for understanding stellar winds as well. In spite of its importance for both space science and stellar physics, basic solar wind properties remain essentially unresolved. Since its discovery about 50 years ago, the complexity of the Sun - corona - solar wind system has complicated the interpretation of observations.

Recent progress in remote sensing observations as provided for example by YOHKOH, SOHO, SPARTAN and ULYSSES as well as some ground based techniques such as Interplanetary Scintillation observations, offer a compelling opportunity to unravel the 50 year old puzzle regarding the heat source or sources that cause the expansion of the solar corona. The new era of solar wind observations initiated by SOHO and ULYSSES, have also led to a wealth of new theoretical approaches.

The goal of the proposed research was to carry out an integrated study of the coronal and solar wind plasma making use of the opportunities provided by the above spacecraft, as well as plasma emission calculations and new ideas on solar wind expansion theory.

1.2 Progress Made

Over the past few years we have carried out, analyzed and made use of a number of different observational and computational techniques to achieve the above goal. Most of the observations were made by instruments on board the SOHO spacecraft. Observations from the Ulysses spacecraft were also intergrated in many of studies.

In particular we focused on the contradictions between results derived from studies of different parts of the solar atmosphere/wind. For example, for the first time a comparison was carried out between electron densities in the lower solar atmosphere (photosphere and chromosphere) which are derived using atmospheric models constrained by observed spectral lines, and the electron densities measured in the corona. Comparing the atmospheric densities to coronal electron densities derived from polarization brightness measurements in the region from about 1.1 to several solar radii, it was shown that there is a discrepancy between

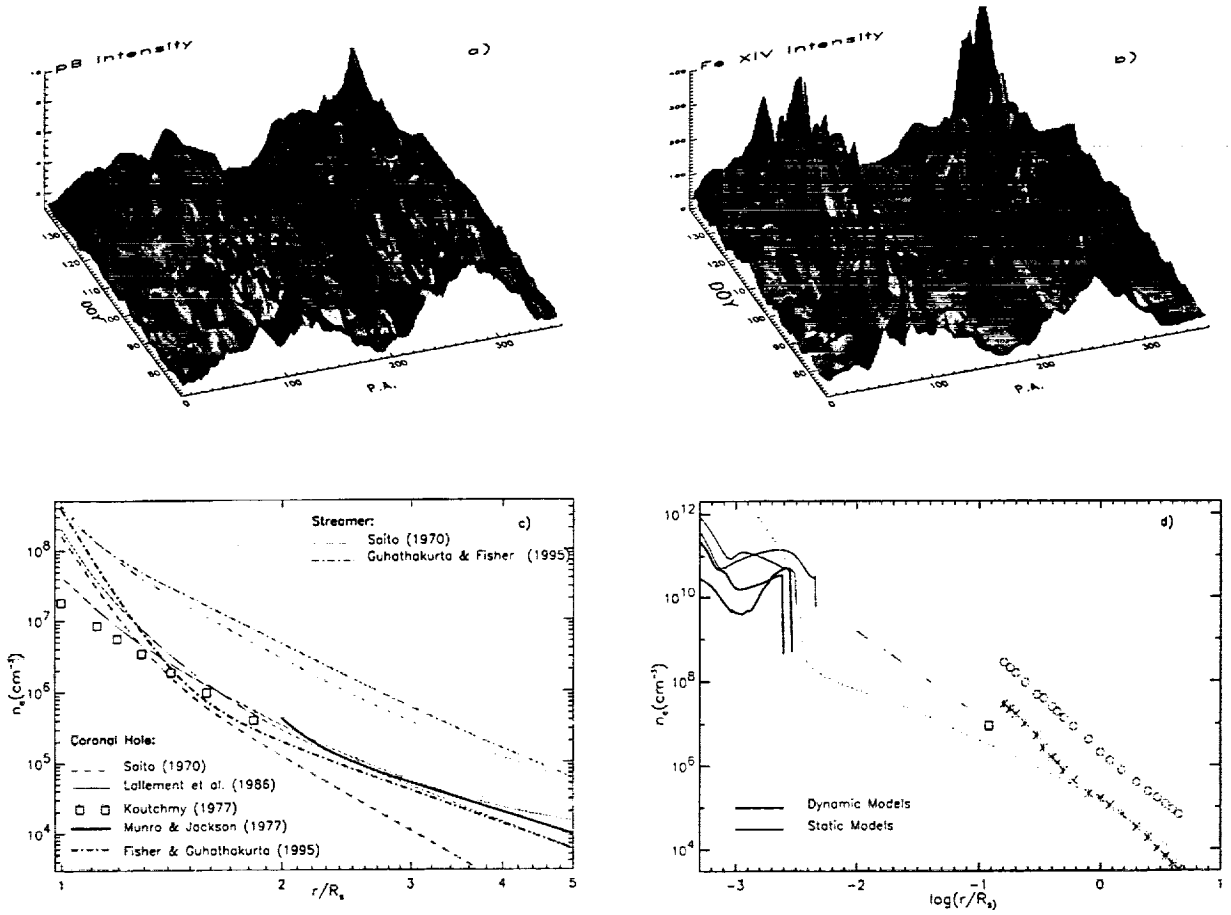

Figure 1: **(a)**: Three dimensional plot of pB intensity measured at 1.16 R_S as a function of time (day of year, DOY), and position angle (P. A.) measured counterclockwise from 0^0 heliographic north. The starting time is DOY 73 in 1993. **(b)** Same as in (a) but for the intensity of the Fe XIV λ5303 spectral line. (c) Electron density as a function of radial distance derived from different eclipse and space-based observations. **(d)** Electron density below log r/R_S = -2.3 (= 1.001 R_S) derived from a number of different chromospheric/transition region models (dynamic models such as Carlson and Stein 1997; and static models such es Fontela, Avrett and Loeser 1990) and spectral line observations. Coronal densities (densities above 1.1 R_S) are the same as in panel (c). The dashed line corresponds to a radial fall off of the chromospheric densities, the dotted line extending from the chromosphere to the corona and solar wind is derived from a theoretical model (Hansteen et al. 1997). For a detailed explanation of these densities see also Esser and Sasselov (1999).

the two sets of densities. The atmospheric electron densities are in agreement with a coronal density of maximum 10^7 cm^{-3} at 1.1 R_S. The pB densities given in the literature are typically 5×10^7 cm^{-3} or higher (see Figure 1). It was shown in the study that this discrepancy which exists regardless of the atmospheric model used, might be due to an overestimation of the electron densities in the corona below 1.5 to 2 R_S (Esser and Sasselov 1999).

Another contradiction that we studies in detail, involves in situ charge state measurements and coronal electron temperatures. It had been a puzzle for quite some time that spectroscopic measurements in the inner corona indicate electron temperatures far too low to produce the ion fractions observed in situ in the solar wind, in particular if the high O VI outflow speeds observed by UVCS are also taken into account (Esser, Edgar and Brickhouse 1998). We were able to show that in order to reconcile the two sets of measurements, a number of conditions have to exist in the inner corona: 1) The electron distribution function has to be Maxwellian or close to Maxwellian at the coronal base; 2) the non-Maxwellian character of the distribution has to develop rapidly as a function of height and has to reach close to interplanetary properties inside of a few solar radii; 3) ions of different elements have to flow with significantly different speeds to separate their "freezing-in" distances sufficiently so they can encounter different distribution functions. We chose a number of different examples to demonstrate that these conditions are general requirements if both coronal electron temperatures and in situ ion fractions are correct. However, these two examples also showed that the details of the required distribution functions are very sensitive to the exact electron temperature, density and ion flow speed profiles in the region of the corona where the ions predominantly form (Esser and Edgar 2000a and b).

We also carried out a number of observations of minor ion spectral lines in the inner corona using the UVCS instrument on SOHO (see Figure 2) (Kohl, Esser et al. 1999; Esser et al. 1999; Kohl et al. 1999). These observations of the Lyman-α 1216 Å, the Mg X 625 Å, and the O VI 1038 Å spectral lines carried out at distances in the range 1.35 to 2.1 R_S in the northern coronal hole, were used to place limits on the turbulent wave motions of the background plasma, and the thermal motions of the protons and Mg^{+9}, and O^{+5} ions. Limits on the turbulent wave motion were estimated from the measured line widths and electron densities derived from white light coronagraph observations assuming WKB approximation at radial distances covered by the observations. It was shown that the contribution of the turbulent wave motion to the widths of the measured spectral lines is small compared to thermal broadening. The observations showed that the proton temperature slowly increases between 1.35 and 2.7 R_S and does not exceed 3×10^6 K in that region. The temperature of the minor ions exceeds the proton temperature at all distances, but the temperatures are neither mass proportional nor mass to charge proportional. It was shown, for the first time, that collision times between protons and minor ions are small compared to the solar wind

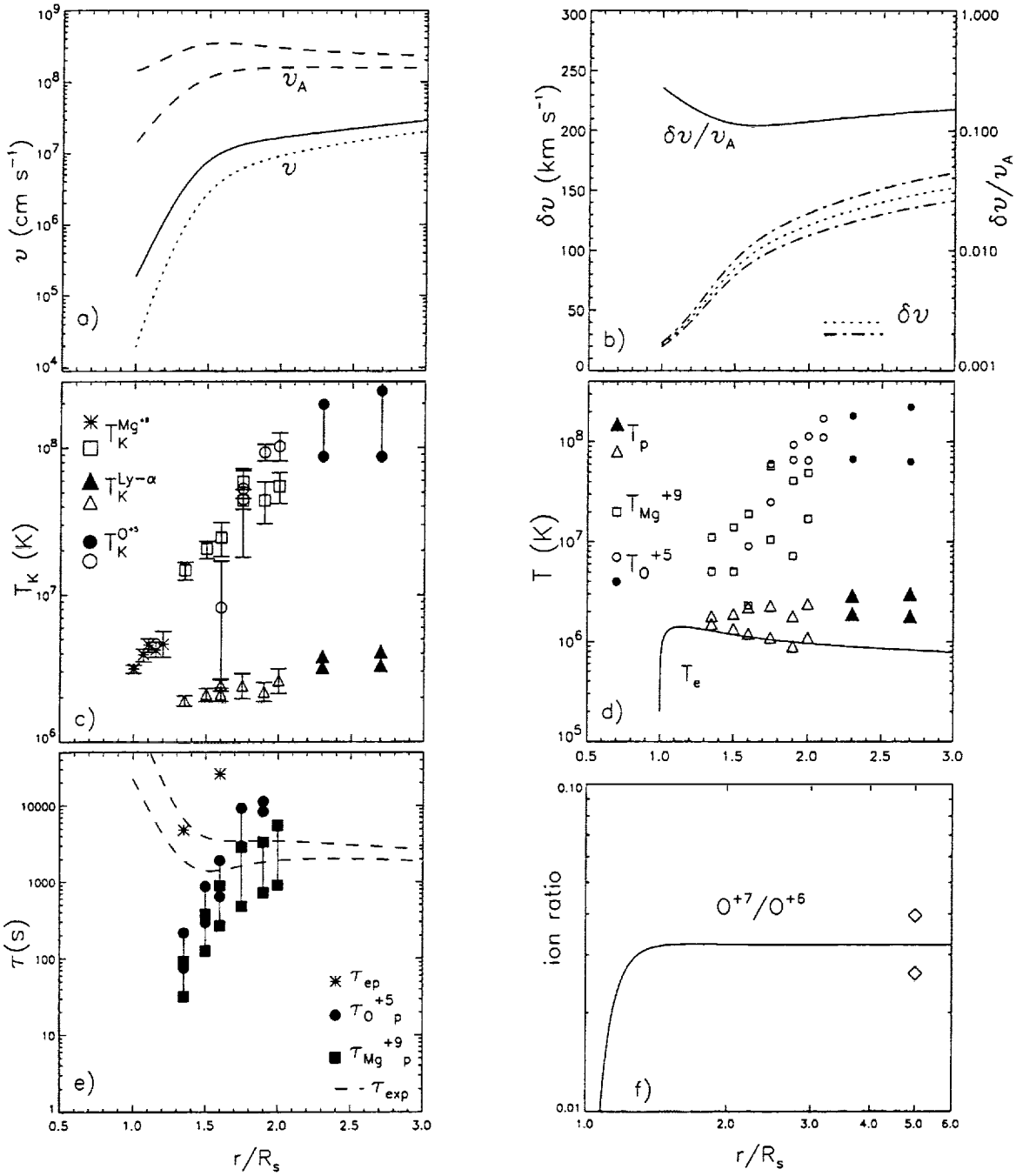

Figure 2: (a) Flow speeds from Fisher and Guhathakurta (1995) coronal electron densities as in Figure 1 (red dots). The flow speeds and densities, together with the assumption of magnetic flux conservation are used to place limits on the Alfvén speed. (b) Limits on the Alfvén wave amplitude (dashed lines) derived from the kinetic ion temperatures in (c) Also shown are corresponding SUMER values (Tu et al. 1998) (dotted line). It is usually assumed that Alfvén waves do not damp if $\delta v/v_A << 1$, which is clearly the case for the distances shown in the figure. (c) UVCS line widths for three different spectral lines, supplemented for Mg X with observations from Hassler et al. (1990). (d) Thermal contribution to the line broadening calculated from (c) and (b). (e) Equipartition times for energy exchange between protons and heavy ions, and proton and electrons, calculated from the densities and temperatures above. Limits on the solar wind expansion times are also shown (dashed lines). (f) Oxygen ion fraction calculated for the same electron densities used in (a), and ion outflow speeds close to the ones in Figure 2d, compared to the observed ULYSSES values (see Esser et al. 1999 for details).

expansion times in the inner corona. At 1.35 R_S the expansion time exceeds the proton Mg^{+9} collision time by more than an order of magnitude. Nevertheless, the temperature of the Mg ions is significantly larger than the proton temperature which indicates that the heating mechanism has to act on time scales faster than minutes. When the expansion time starts to exceed the collision times a rapid increase of the O^{+5} ion spectral line width is seen. This indicates that the heavier and hotter ions lose energy to the protons as long as collision frequencies are high, and that the ion spectral line width increases rapidly as soon as this energy loss stops.

Some earlier theoretical studies focused on the properties of protons in the solar wind (Li et al. 1999a and b). However, to study the properties of the minor ions we presented, for the first time, a one-dimensional, four-fluid turbulence-driven solar wind model in order to investigate the preferential acceleration and heating of heavy ions by the resonant cyclotron interaction with parallel-propagating left-hand-polarized ion cyclotron waves. The model contains four species: electrons, protons, alpha particles, and one species of minor ions. A Kolmogorov type of cascade effect is introduced to transfer energy from the low-frequency Alfvén waves to the high-frequency ion cyclotron waves, which are assumed to be entirely dissipated by the wave-particle interaction. The quasi-linear theory of the wave-particle interaction is invoked to distribute the dissipated wave energy among the three ion species based on a given power law spectrum of the ion cyclotron waves and the cold plasma dispersion relation. It was found that in terms of the cold plasma dispersion relation, the dispersion generated by all ion species has an appreciable influence on both the behavior of the major species and the preferential acceleration and heating of the minor ions. The larger the number of species included in the dispersion relation is, the stronger preferential acceleration and heating produced by the waves for the heavy ions close to the Sun will be. A detailed comparison was carried out between two cases, one with and the other without the dispersive effect of the minor ions. Although the solutions for the two cases are somewhat different, they predict a more or less similar behavior of the minor ions, which essentially agrees with the above minor ion observations. This indicates that the resonant cyclotron interaction may be responsible for the preferential acceleration and heating of minor ions in the fast solar wind. Furthermore, the influence of minor ions on the proton-alpha solar wind is found to be dominated by the dispersive effect of the minor ions. Even though such an influence is exaggerated by the cold plasma dispersion relation, it is still small and remains within the present observational uncertainties. Therefore minor ions may be treated approximately as test particles in the solar wind. A comparison between the UVCS observations and the model results is shown in Figure 3 (from Hu, Esser and Habbal 2000).

We also examined the accuracy of a common FIP effect diagnostic, the ratio of Ne VI to Mg VI lines in the solar transition region. Since the two ions have quite similar contribution

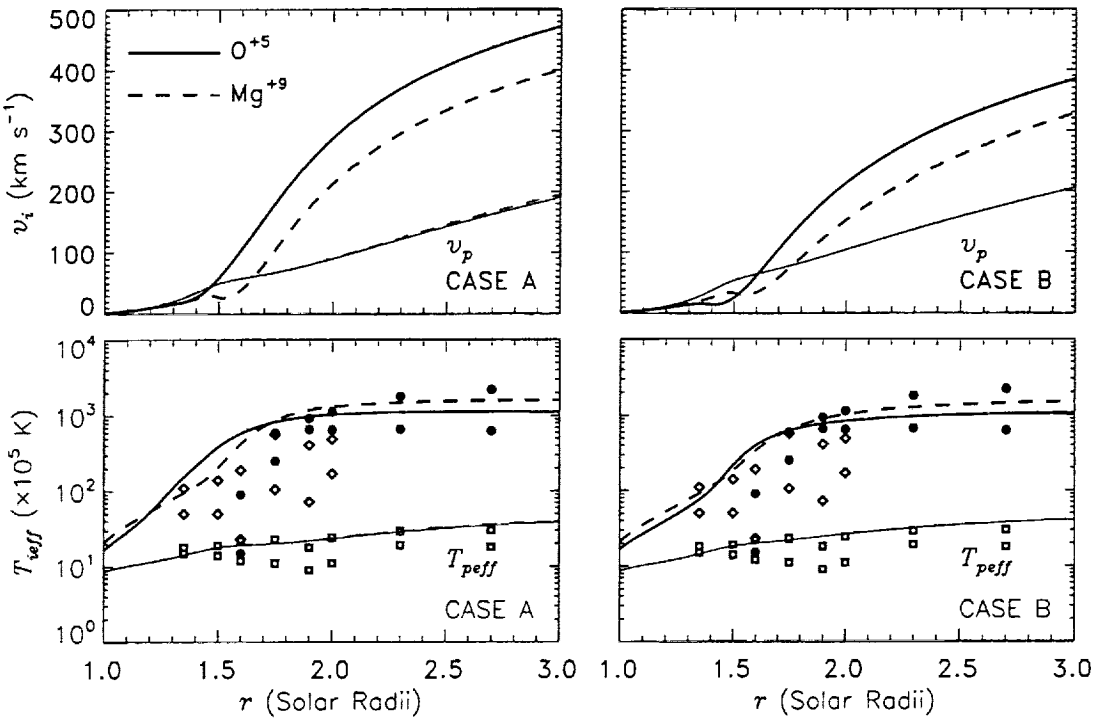

Figure 3. Radial velocity and effective temperature profiles for the O^{+5} and Mg^{+9} ions in the range of 1-3 R_s. Cases A and B are associated with dispersion relations (23a) and (23b) respectively. The observed effective temperatures reported by *Esser et al.* [1999] are shown for the protons (open squares), O^{+5} ions (solid circles), and Mg^{+9} ions (open rhombuses) in the lower panels.

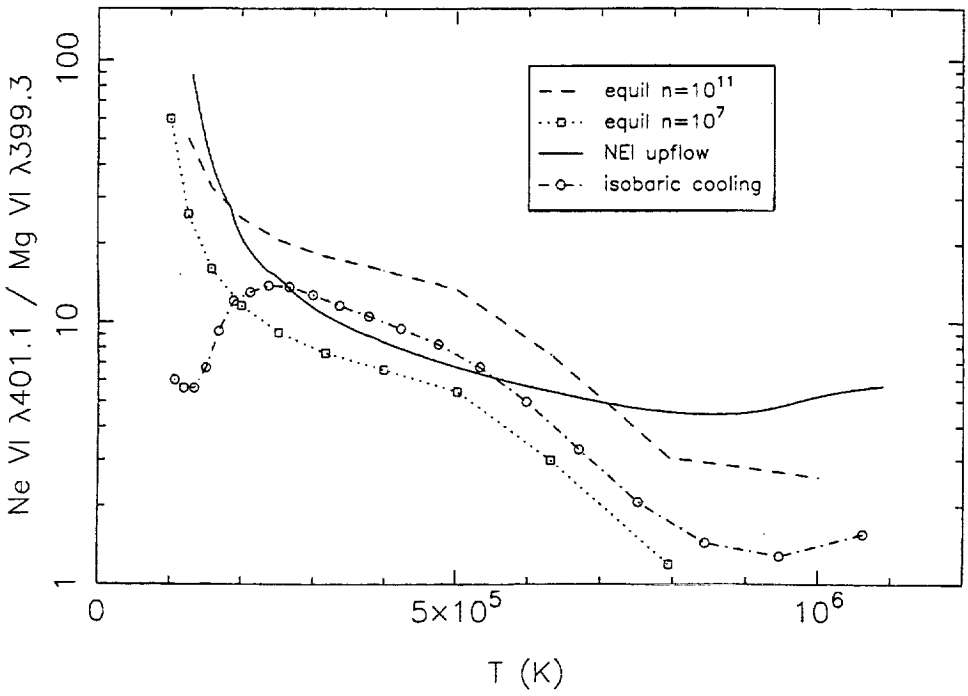

Figure 4. Ratio of Ne VI λ401.1/Mg VI λ399.3 line emissivities for coronal equilibrium at two densities, for isobaric cooling case, and for the upflow model of Hansteen et al. (1997). The figure clearly shows that density as well as non-equilibrium effects can alter the line ratio, and that a temperature effect is also present.

functions near their maxima in equilibrium, the ratio of these two ions is often taken to be the abundance ratio of Ne and Mg. First we computed non-equilibrium ionization effects on the ratio of ion fractions for a variety of simple flows through the transition region. Calculating the spectral line ratios for a few examples, we then showed that non-equilibrium effects as well as temperature and density dependence must be evaluated for each line ratio used in the diagnostics (see Figure 4, from Edgar and Esser 2000).

Even though most of our studies focused on the high speed solar wind, we carried out some investigations regarding the boundaries between coronal holes and adjacent regions (Young and Esser 1999a and b; Esser 1999; Kaghashvili and Esser 1999 and 2000). These studies focused on the observational properties of the boundary regions, except for the paper by Kaghashvili and Esser in which it was shown that the presence of differential flow speeds could lead to a conversion of Alfvén waves which are difficult to damp in the inner corona to fast mode waves which are easily damped and could provide a heating of the electrons in the inner corona.

The lastest work partially supported by this grant was a set of UVCS observations of a coronal mass ejection. These observations are still being analyzed.

2. Publications in Journals and Proceedings Funded or Partially Funded by Grant NAG5-6192

1. Y. Yamauchi, T. Tokumaru, M. Kojima, P. K. Manoharan, and R. Esser, Study of density fluctuations in the solar wind acceleration region, *J. Geophys. Res.*, **103**, 6571, 1998.

2. R. Esser, R. J. Edgar, and N. S. Brickhouse, High minor ion outflow speeds in the inner corona and observed ion charge states in interplanetary space, *Astrophys. J.*, **498**, 448, 1998.

3. X. Li, S. Habbal, J. Hollweg and R. Esser, Heating and Cooling of protons by turbulence-driven ion cyclotron waves in the fast solar wind, *J. Geophys. Res.*, **104**, 2521, 1999a.

4. X. Li, S. Habbal, J. Hollweg and R. Esser, Proton temperature unisotropy in the fast solar wind, in Proceedings of SW9 conference, *AIP*, **471**, 531, 1999b.

5. R. Esser, S. Fineschi, D. Dobrzycka, S. R. Habbal, R. J. Edgar, J. C. Raymond, J. L. Kohl, and M. Guhathakurta, Plasma properties in coronal holes derived from measurements of minor ion spectral lines and polarized white light intensity, *Astrophys. J. Lett.*, **510**, L64, 1999.

6. J. L. Kohl, R. Esser, S. R. Cranmer, S. Fineschi, L. D. Gardner, A. V. Panasyuk, L. Strachan, R. M. Suleiman, R. A. Frazin, and G. Noci, EUV spectral line profiles in polar coronal holes from 1.3 to 3.0 R_S, *Astrophys. J. Let.*, **510**, L59, 1999.

7. R. Esser, Coronal hole boundaries and interactions with adjacent regions, *Space Sci. Rev.*, **87**, 93, 1999.

8. R. Esser and D. Sasselov, On the discrepancy between atmospheric and coronal electron densities, *Astrophys. J. Lett.*, **521**, L145, 1999.

9. P. Young and R. Esser, Comparing quiet sun and coronal hole regions with CDS/SOHO, *Space Sci. Rev.*, **87**, 245, 1999a.

10. P. Young and R. Esser, Temperature and density in coronal holes - results from CDS/SOHO, in Proceedings of SW9 conference, *AIP*, **471**, 273, 1999b.

11. J. L. Kohl, S. Fineschi, R. Esser, A. Ciaravella, S. R. Cranmer, L. D. Gardner, R. Suleiman, G. Noci. and A. Modigliani, UVCS/SOHO observations of spectral line profiles in polar coronal holes, *Space Sci. rev.*, **87**, 233, 1999.

12. E. Kaghashvili and R. Esser, Shear velocity induced conversion of Alfvén waves, in Proceedings of SW9 conference, *AIP*, **471**, 341, 1999.

13. C. Halas Wood, S. Habbal, R. Esser, M. Penn, and D. McKenzie, Inferences of plasma parameters in coronal holes, in Proceedings of SW9 conference, *AIP*, **293**, 1999.

14. Y. Yamauchi, M. Tokumaru, M. Kojima, P. Manoharan, and R. Esser, Radial evolution of micro-turbulence in the solar wind observed with interplanetary scintillation, in Proceedings of SW9 conference, *AIP*, **471**, 473, 1999.

15. R. Esser and R. J. Edgar, Reconciling spectroscopic electron temperature measurements

in the inner corona with in situ charge state measurements, *Astrophys. J. Lett.*, **532**, 71, 2000a.
16. Esser, R., and R. J. Edgar, Constraints on ion outflow speeds and electron distribution function in the corona derived from SUMER electron temperatures and SWICS ion fractions, Adv. Space Res., submitted, 2000b.
17. Y.-Q. Hu, R. Esser and S. R. Habbal, A four-fluid turbulence-driven solar wind model for preferential acceleration and heating of heavy ions, *J. Geophys. Res.*, **105**, 5093, 2000.
18. E. Kaghashvili and R. Esser, Shear induced mode conversion in solar wind and streamer plasmas, *Astrophys. J.*, **539**, 463, 2000.
19. R. Esser, Solar wind acceleration, in *Encyclopedia of Astronomy and Astrophysics*, 2000.
20. R. Edgar and R. Esser, Non-equilibrium ionization and FIP effect diagnostics, *Astrophys. J. Lett.*, **534**, L37, 2000.